

# Type 1 Choroidal Neovascularization Lesion Size: Indocyanine Green Angiography Versus Optical Coherence Tomography Angiography

Eliana Costanzo,<sup>1,2</sup> Alexandra Miere,<sup>1</sup> Giuseppe Querques,<sup>1,3</sup> Vittorio Capuano,<sup>1</sup> Camille Jung,<sup>1</sup> and Eric H. Souied<sup>1</sup>

<sup>1</sup>Department of Ophthalmology, University Paris Est Créteil, Centre Hospitalier Intercommunal de Créteil, Créteil, France

<sup>2</sup>Department of Ophthalmology, Second University of Naples, Naples, Italy

<sup>3</sup>Department of Ophthalmology, University Scientific Institute San Raffaele, Milan, Italy

Correspondence: Eric H. Souied, Department of Ophthalmology, Centre Hospitalier Intercommunal de Créteil, Université de Paris Est Créteil, 40 Avenue de Verdun, 94000 Créteil, France; eric.souied@chicreteil.fr.

Submitted: December 9, 2015

Accepted: April 17, 2016

Citation: Costanzo E, Miere A, Querques G, Capuano V, Jung C, Souied EH. Type 1 choroidal neovascularization lesion size: indocyanine green angiography versus optical coherence tomography angiography. *Invest Ophthalmol Vis Sci*. 2016;57:OCT307–OCT313. DOI:10.1167/iovs.15-18830

**PURPOSE.** To evaluate the size of type 1 choroidal neovascularization (CNV) in neovascular AMD by optical coherence tomography angiography (OCTA) and to compare with indocyanine green angiography (ICGA).

**METHODS.** Patients diagnosed type 1 CNV underwent multimodal imaging by fluorescein angiography (FA), ICGA, spectral-domain (SD)-OCT, and OCTA. Lesion size was measured both on OCTA at the choriocapillaris level with “select area” and “vessel area” functions, incorporated in AngioVue software and on ICGA at intermediate and late phases, by two masked independent readers.

**RESULTS.** Nineteen eyes of 17 patients (mean age  $80.6 \pm 8.36$ ) were included in the analysis. Mean visual acuity was 0.2 logMAR. All OCTA revealed a high flow neovascular network in the choriocapillaris segmentation. On OCTA, interclass correlation between readers 1 and 2 was 0.96 (95% confidence interval [CI] 0.94–0.99) for select area and 0.97 (95% CI 0.96–0.99) for vessel area. The difference between lesion size in OCTA versus ICGA was detected in all eyes and it was statistically significant for both readers ( $P < 0.05$ ).

**CONCLUSIONS.** Optical coherence tomography angiography provides both quantitative and qualitative information on type 1 CNV and appears as a new reproducible way to evaluate CNV area and vessels area. Type 1 CNV lesion size in the choriocapillaris segmentation of OCTA and ICGA intermediate and late phases revealed that the OCTA size is significantly smaller than the ICGA size. This supports the idea that OCTA could be considered for evaluation of the neovascular lesion and for evaluation of therapeutic responses.

**Keywords:** age-related macular degeneration, type 1 choroidal neovascularization, optical coherence tomography angiography, indocyanine green angiography

Exudative AMD is defined as abnormal growth of neovascular tissue from the choriocapillaris through or beneath the retinal pigment epithelium (RPE).<sup>1,2</sup> Gass described three histologic forms of choroidal neovascularization (CNV): type 1 CNV, located beneath RPE monolayer and above the Bruch's membrane; type 2 CNV, located above the RPE monolayer; combined type 1 and type 2 CNV.<sup>3</sup> The most frequent phenotype of exudative AMD is type 1 CNV.<sup>4</sup> While fundus ophthalmoscopy of type 1 CNV shows nonspecific signs such as drusen or pigmentary alterations of RPE, subretinal fluid (SRF), hard exudates, and possibly hemorrhages, multimodal imaging provides an accurate description of the features and extension of the choroidal new vessels.<sup>5</sup> Type 1 CNV corresponds angiographically to occult, ill defined, neovascularization, described as an ill-defined lesion in fluorescein angiography (FA).<sup>5,6</sup> The detection of CNV was improved using indocyanine green angiography (ICGA), as demonstrated by Yannuzzi.<sup>7</sup>

As multimodal imaging provides a better understanding of type 1 neovascularization,<sup>8,9</sup> combined FA, ICGA, and spectral-domain optical coherence tomography (SD-OCT) play a key

role in the diagnosis of type 1 CNV. On FA, type 1 CNV is epitomized as a heterogeneous hyperfluorescence with late moderate leakage, situated in the macular region and associated with a pigment epithelial detachment (PED) and stippled hyperfluorescent dots.<sup>6</sup> Moreover, despite the enhanced visualization of the entire neovascular membrane on ICGA,<sup>6,7,10,11</sup> FA is the wider used for CNV detection.<sup>12</sup> Several patterns of ICGA hyperfluorescence have been observed, including early-appearing small hyperfluorescent spots (hot spots), plaque-like hyperfluorescence, and late-appearing hyperfluorescence with indistinct edges or a combination of these patterns.<sup>13</sup> Furthermore, on SD-OCT type 1 CNV is indicated by a PED (98% of cases), which takes the form either of a limited RPE elevation (35.3%) or of a complete RPE detachment (62.7%).<sup>8</sup> The presence of choroidal neovascularization harbors the aspect of a hyperreflective area in contact with the RPE monolayer, detected in 62.7% of eyes. Serous retinal detachment (SRD) frequently accompanies active neovascular membranes, in the form of SRF, intraretinal cystic spaces or diffuse neurosensory infiltration.<sup>8,14,15</sup> Evaluation of lesion using these imaging techniques is difficult in a clinical setting due



to limits such as leakage on FA or low feasibility of ICGA examination at each visit. Optical coherence tomography angiography (OCTA) is a depth-resolved imaging technique that uses the split spectrum amplitude decorrelation angiography (SSADA) to generate amplitude angiography images. It allows blood flow visualization and thus a quantitative and, to a greater extent, qualitative assessment of CNV. Type 1 CNV is revealed, in OCTA, by a high flow, well organized vascular network appearing in the outer retinal/choriocapillaris segmentations, with a distinguishable feeder vessel in almost all cases.<sup>16-18</sup>

The difference between angiographic pattern on the two imaging techniques (OCTA and ICGA) resides on the different concept applied for each examination. While OCTA allows visualization of nonstatic tissues, blood cell flow, by measuring the variation in reflected OCT signal amplitudes between sequential cross-sectional scans, indocyanine green binds almost completely to plasma proteins (predominantly globulins and, to a smaller percentage, alpha-lipoproteins, and albumins).<sup>19</sup> This influences essentially the final angiographic images: on OCTA the images will be depth resolved and time-independent, while on ICGA leakage will occur slowly from the fenestrated choriocapillaris. The ICG-protein complex will be slowly reabsorbed into circulation, which is why gradual impregnation of the choroid occurs in time in ICGA, causing hyperfluorescence in the late frames of the examination.<sup>20,21</sup>

Our study tries to highlight the sensitivity evaluation of type 1 CNV lesion size on OCTA, which is able to clearly delineate CNV margins when, compared with invasive, time-consuming techniques like ICGA.

## METHODS

### Study Population

In this prospective study, we studied consecutive patients presenting at the University Eye Clinic of Créteil (Créteil, France), with type 1 choroidal neovascularization (CNV) in the context of neovascular AMD. The study was performed in agreement with the Declaration of Helsinki for research involving human subjects and the French legislation. French Society of Ophthalmology institutional review board approval was obtained for this study.

All patients satisfied the inclusion criteria for the diagnosis of type 1 CNV in multimodal imaging (Spectralis HRA+OCT; Heidelberg Engineering, Heidelberg, Germany): the presence of PED with or without SRD on SD-OCT, hyperfluorescent pinpoints on late times of FA, neovascular network visualization on intermediate<sup>20-22</sup> phase of ICGA, and a late hypercyanescent plaque on ICGA.

Patients with one or more of the following clinical conditions were excluded from the study: important media opacities, evidence of diabetic retinopathy or any other macular or retinal vascular disease, subretinal fibrosis, other vitreoretinal disease, previous treatment by laser photocoagulation, intravitreal injections of steroids, retinal surgery, signs or history of central serous chorioretinopathy, and hereditary retinal dystrophy. Patients with poor quality images in OCTA (i.e., due to eye movement) or with a lesion that exceeded the  $3 \times 3$  scanning area, were not included in the analysis.

### Study Protocol

All patients underwent a complete ophthalmic examination including monocular best-corrected visual acuity (BCVA) using standard Early Treatment Diabetic Retinopathy Study (ETDRS) charts, slit-lamp examination, and fundus biomicroscopy. All

eyes underwent FA, ICGA, infrared reflectance imaging (IR), and simultaneous SD-OCT imaging using a Spectralis OCT (Heidelberg Engineering), as well as OCTA (AngioVue, RTVue XR Avanti; Optovue, Inc., Fremont, CA, USA).<sup>15,17</sup> Optical coherence tomography angiography examinations were performed by two trained examiners (EC, AM) after pupil dilation. The instrument used for OCTA images is based on the Optovue RTVue XR Avanti (Optovue, Inc.) to obtain amplitude decorrelation angiography images. This instrument has an A-scan rate of 70,000 scans per second, using a light source centered on 840 nm and a bandwidth of 50 nm. Each OCTA volume contains  $304 \times 304$  A-scans with two consecutive B-scans captured at each fixed position before proceeding to the next sampling location. Split-spectrum amplitude-decorrelation angiography was used to extract the OCTA information. Each OCTA volume is acquired in 3 seconds and two orthogonal OCTA volumes were acquired in order to perform motion correction to minimize motion artifacts arising from microsaccades and fixation changes. Angiography information displayed is the average of the decorrelation values when viewed perpendicularly through the thickness being evaluated.

To evaluate the architectural changes of the retinal microvascular network in eyes with type 1 CNV we used a  $3 \times 3$  scanning area. Minor adjustments of the segmentation provided by the machine software were made, in order to overcome various artifacts, such as projection artifact, motion artifact or segmentation errors,<sup>23</sup> and thus to ensure a correct visualization of the outer retinal layers and choriocapillaris. The OCTA findings were then carefully compared to FA and ICGA findings, as well as to SD-OCT findings, by two expert retinal specialists (GQ, EHS). Furthermore, lesion area was measured on ICGA and OCTA using the proprietary software embedded in Spectralis (Heidelberg Engineering) and Optovue RTVue XR Avanti (Optovue, Inc.), respectively.

To measure the type 1 CNV lesion size on ICGA we used the area-measuring software provided by Spectralis. Classically, early ICGA phase corresponds to a not yet filled retinal artery, intermediate phase is defined by the filling of both arteries and veins, and the late phase corresponds to more than 10 minutes after injection.<sup>20</sup> Consequently, two frames of ICGA were taken into account: the venous intermediate frame<sup>20</sup> (between 3 and 5 minutes, mean 3.4 minutes  $\pm 0.75$ ) and the late frame (between 30 and 35 minutes, mean 31.2 minutes  $\pm 0.93$ ). Choroidal neovascular edges were manually contoured followed by a surface area computation with the software. Two masked retina experts (GQ and EHS) measured the ICGA lesion size in all patients independently; in case of discordance the measurements were reevaluated by a third retinal specialist (VC).

In order to measure the type 1 CNV lesion size on OCTA we used the AngioAnalytics System provided by AngioVue software (AngioVue, RTVue XR Avanti; Optovue, Inc.), by selecting the "Flow Area" function; this function allows the quantification of a user-defined vascular area at the automatic segmented choriocapillaris layer, followed by an automatic computation of "select area" and "vessel area." The "select area" feature corresponds to the total area manually contoured with the flow area draw tool, while the "vessel area" feature corresponds to the total area of solely vessels with detectable flow, as determined by AngioVue software within the user-defined region. This user-defined region was automatically yellow-colored. Likewise, two masked trained users (EC and AM) measured the OCTA neovascular lesion size in all patients independently; in case of discordance the measurement were evaluated by a third trained user (VC). Discordance between the independent measurements of the two observers was defined as a difference of more than 10% of the lesion area.

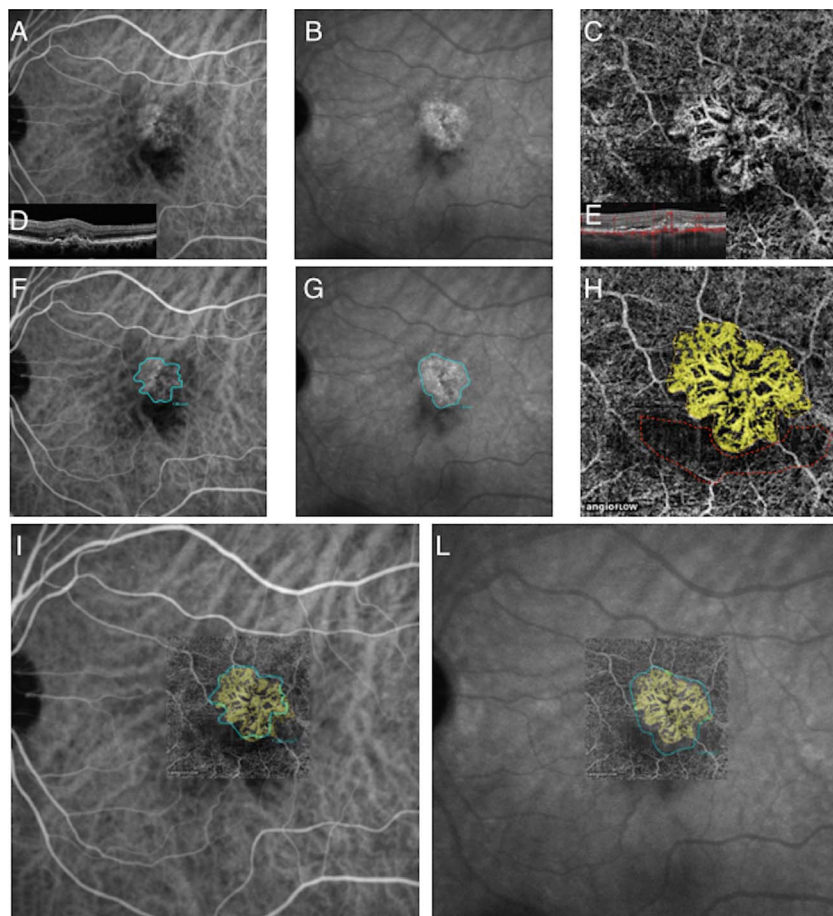


**FIGURE 1.** Type 1 neovascularization in AMD: ICGA versus OCTA imaging. Case #16: 87-year-old male patient, BCVA 20/32, treatment-naïve. (A) Indocyanine green angiography intermediate-phase reveals a hypercyanescent subfoveal lesion (4'). (B) Indocyanine green angiography late-phase shows the same lesions, with enhanced contrast (33'). (C) Optical coherent tomography angiography automatic segmented choriocapillaris layer; note the high flow, "seafan" pattern neovascular complex. (D) Spectral-domain (SD) OCT imaging reveals a type 1 lesion. (E) Coregistered OCT B-scan image that shows the level of choriocapillaris segmentation. (F) Lesion's size on ICGA intermediate-phase, the neovascular membrane, encircled in *blue* using the "surface area measuring" system, measures 1.60 mm<sup>2</sup>. (G) Lesion's size on ICGA late-phase, the neovascular membrane, encircled in *blue* using the "surface area measuring" system, measures 2.02 mm<sup>2</sup>. (H) Lesion's size on OCTA choriocapillaris layer: in yellow the neovascular complex size computing by AngioAnalytic System, select area: 1.562 mm<sup>2</sup>, vessel area: 0.996 mm<sup>2</sup>; *red dashed lines* contour a hypoperfused area of the choriocapillaris adjacent to the neovascular complex. (I) Overlay of OCTA choriocapillaris layer on intermediate-phase of ICGA; note the almost perfect correspondence of the lesion's margins on OCTA and ICGA. (L) Overlay of OCTA choriocapillaris layer image on late-phase of ICGA; note that the edges of contoured neovascular complex on ICGA is larger than the OCTA lesion.

We performed OCTA and ICGA overlay, using Mac OSx Keynote (version 6.5.2, 2015; Apple, Inc., Cupertino, CA, USA). Optical coherence tomography angiography 3 × 3 mm images of the choriocapillaris segmentation, previously measured, were overlapped on the measured intermediate and late ICGA frames. In order to correctly overlay the images, we used a transparency tool and carefully adjusts the OCTA image size to major vascular contours (Figs. 1I, 1L, 2F, 2G). After performing image overlay, all OCTA lesions with edges that exceeded the 3 × 3 scanning area were excluded from the analysis, in order to have a reliable measurement of the neovascular membrane in both imaging techniques.

### Statistical Analysis

The analysis included descriptive statistics for demographics and main clinical data and qualitative descriptions of the imaging characteristics. Qualitative variables were described in percentages and quantitative variables were described by their mean with SD or by their median with interquartile range. Comparisons of medians were performed using the Wilcoxon

signed-rank test. Bland Altman and intraclass correlation were used to evaluate the agreement between the readers and between the methods. *P* less than 0.05 were retained as significant.

### RESULTS

Nineteen eyes of 17 patients met the inclusion criteria and were taken into account for data analysis. The characteristics of study population were: mean age 80.6 (±8.36) years, 7 female and 10 male, with a mean BCVA of 0.2 logMAR (from 20/80 to 20/20 Snellen); 11 eyes were treatment-naïve, while 8 eyes were previously treated by anti-VEGF. The treated group had a mean of 7.65 (± 16) intravitreal injections. Spectral-domain OCT revealed the presence of PED in 100% of cases (19/19 eyes), SRF in 68.4% of cases (13/19 eyes) and intraretinal fluid in 15.8% of cases (3/19 eyes).

On OCTA, the neovascular lesion morphology corresponded to either "medusa" pattern, in which vessels are radiating in all directions from the center of the lesion (7/19 eyes, 36.8%), "seafan" pattern, in which vessels are radiating from one side

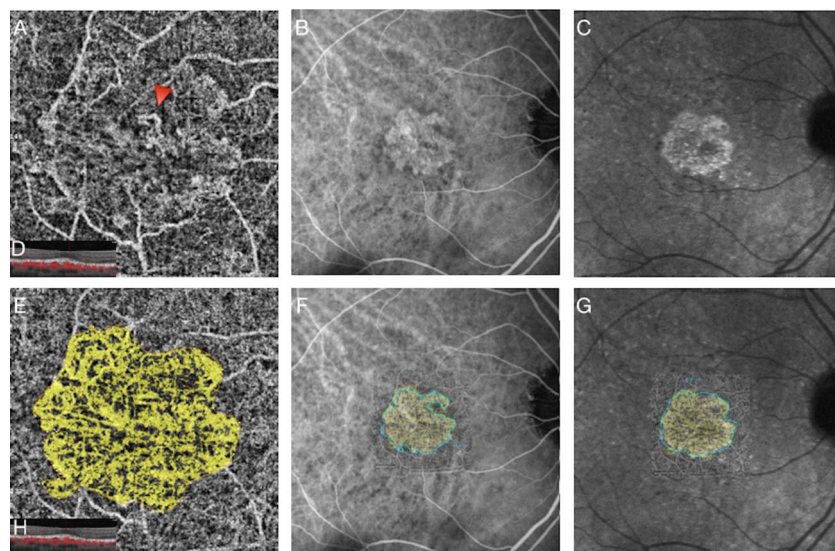


**FIGURE 2.** Example of similar size of type 1 neovascular lesion, measured by OCTA and ICGA. Case #18: 87-year-old male patient, BCVA 20/20, status post three anti-VEGF intravitreal injections. (A) Optical coherent tomography angiography automatic segmented choriocapillaris layer; note the high flow neovascular complex with a thick central trunk probably corresponding to a feeder vessel (red bead arrow). (B) Indocyanine green angiography intermediate-phase (5') shows the hypercyanescent neovascular lacy harboring well-defined borders. (C) Indocyanine green angiography late-phase (34') that shows the hypercyanescent plaque. (D) Coregistered OCT B-scan, related to *image a*, that shows the level of choriocapillaris segmentation. (E) Lesion's size on OCTA choriocapillaris layer: in yellow the neovascular complex size computing by AngioAnalytic System, select area: 3.23 mm<sup>2</sup>, vessel area: 2.09 mm<sup>2</sup>. (H) Coregistered OCT B-scan image that shows the level of choriocapillaris segmentation. (F, G) Overlay of OCTA choriocapillaris layer on intermediate and late-phase of ICGA, 3.21 and 3.33 mm<sup>2</sup>, respectively; note the perfect correspondence of the lesion's margins on OCTA and both intermediate and late phases of ICGA.

of the lesion (3/19 eyes, 15.8%), or an indistinct pattern (9/19 eyes, 47.4%). Figures 1 and 2 show examples of computing results in a treatment-naïve patient and in a treated patient, respectively. On ICGA, type 1 CNV mean area measurement in the intermediate phase was 2.70 mm<sup>2</sup> ( $\pm$  2.43) for reader 1 and 2.71 mm<sup>2</sup> ( $\pm$  2.45) for reader 2, while in late phase it was 3.04 mm<sup>2</sup> ( $\pm$  2.38) and 2.92 mm<sup>2</sup> ( $\pm$  2.55), respectively. On OCTA, type 1 CNV size on choriocapillaris automatic segmentation, measured with select area was 2.21 mm<sup>2</sup> ( $\pm$  2.15) for reader 1 and was 2.03 mm<sup>2</sup> ( $\pm$  1.92) for reader 2, while the vessel area was 1.17 mm<sup>2</sup> ( $\pm$  1.10) and 1.11 mm<sup>2</sup> ( $\pm$  0.99), respectively. In all eyes, the overlay of the 3  $\times$  3 mm scanning area from OCTA to ICGA images revealed a lesion smaller on OCTA than both intermediate and late ICGA. There was complete agreement for the results obtained by OCTA and multimodal evaluation for all eyes. Figure 3 shows an example of an independent size evaluation for two different readers. Interclass correlation (ICC) between readers 1 and 2 was evaluated. Interclass correlation was 0.96 (confidence interval [CI] 95% was 0.94–0.99) for select area and 0.97 (CI 95% 0.96–0.99) for vessel area. Interclass correlation between readers 1 and 2 for ICGA was 0.99 for intermediate phase (CI 95% 0.98–0.99) and 0.98 for late phase (CI 95% 0.96–0.99). The Table shows the statistical analysis results and the lesion size comparison between OCTA and ICGA, using a Wilcoxon signed rank test: for both readers all compared variables were statistically significant ( $P < 0.05$ ). For each reader we compared the lesion size measured on OCTA as “vessel area” and “select area” with the lesion size measured on ICGA both in intermediate and late phases. The comparison between “vessel area” and the lesion measured on intermediate and late times of ICGA was statistically different ( $P = 0.0001$ ) for both readers. The comparison between “select area” and the lesion size on intermediate times of ICGA was statistically significant for both readers,  $P = 0.02$  for reader 1 and  $P = 0.002$  for reader 2. The comparison between “select area” and lesion size in late phase of ICGA have  $P = 0.0003$  and  $P = 0.0005$  for reader 1 and

reader 2, respectively. We also analyzed the difference between the lesion size measured on intermediate and late phase of ICGA that resulted statistically significant only for one reader ( $P = 0.08$  and  $P = 0.15$ , respectively).

## DISCUSSION

Since the 1990, ICGA has been widely used to assess type 1 CNV,<sup>7,18</sup> known for their ill-defined aspect on FA.<sup>5,6</sup> Specific properties of indocyanine green dye allow visualization, in ICGA, of the deep chorioidal vasculature, and thus the study of occult membranes.<sup>7,11,14,24–26</sup> Moreover, Reichel et al.<sup>10</sup> demonstrated the use of ICGA in eyes with hemorrhage obscuring CNV visualization. Recently, Rush et al.<sup>25</sup> have shown that a decrease of greater than or equal to 33% at 2 months was associated with an important decrease in CNV size at 12 months, offering both interesting prognostic information at a more personalized treatment strategy. Moreover, staining on ICGA does not always correlate to the neovascular membrane and the staining can be inconsistent after anti-VEGF therapy and can persist after CNV regression.<sup>25,26</sup> Despite these evidences, the limits of ICGA are well-known<sup>6,21,26</sup>: ICGA is an invasive imaging technique and, though its side-effects are milder than those of FA, ICG is iodine based, which contraindicates it in patients with iodine allergy or seafood allergy due to cross-reaction.<sup>27</sup> Furthermore, Ho et al.<sup>28</sup> suggested the possibility of a diffusible chorioidal source of leakage of indocyanine green dye. Comparing FA and ICGA, only the 60% of type 1 CNV are correctly localized on FA.<sup>6</sup> Furthermore, ICGA is a 30 minutes examination,<sup>20,21</sup> much longer than OCTA.

These facts led us to analyze type 1 CNV lesion size in ICGA and OCTA. Optical coherence tomography angiography is a non-dye technique that allows an in-depth analysis of the macula, generating a direct visualization of the vascular anomalies that cannot be seen otherwise. However, OCTA

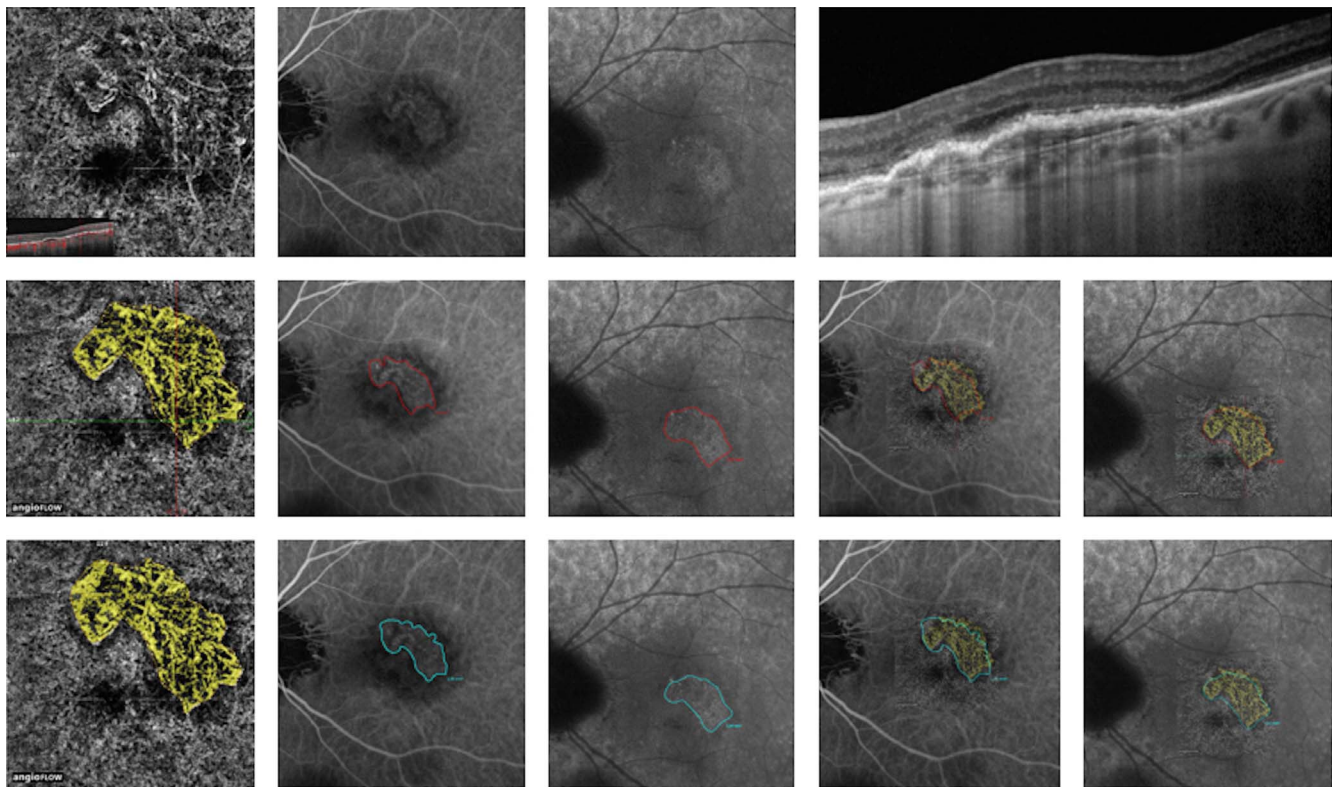


**FIGURE 3.** Example of interusers agreement for measurement of type 1 neovascular lesions. Case #6: 75-year-old male patient, visual acuity 20/50, status post six anti-VEGF intravitreal injections. *Top panel* (from left to right): OCTA automatic segmented choriocapillaris layer that shows a high flow neovascular complex with a central feeder vessel, vessels radiating in all directions in a “medusa” pattern and a hypoperfused area contouring the lesion; intermediate-phase (4’) ICGA image that reveals the hypercyanescent neovascular plaque, ill defined; SD-OCT shows the fibrovascular PED. *Middle panel* (from left to right) reader 1: OCTA select area: 1.901 mm<sup>2</sup>, vessel area: 0.982 mm<sup>2</sup>; intermediate-phase ICGA lesion size was 2.26 mm<sup>2</sup>, late-phase ICGA lesion size was 2.51 mm<sup>2</sup>; overlay of choriocapillaris OCTA layer on intermediate-phase of ICGA, overlay of choriocapillaris OCTA layer on late-phase of ICGA on the right. *Bottom panel* (from left to right) reader 2: OCTA select area: 1.910 mm<sup>2</sup>, vessel area: 1.041 mm<sup>2</sup>; intermediate-phase ICGA lesion’s size 2.30 mm<sup>2</sup>, late-phase ICGA lesion’s size 2.24 mm<sup>2</sup>. On the *right*, overlay of choriocapillaris OCTA layer on intermediate-phase of ICGA, overlay of choriocapillaris OCTA layer on late-phase of ICGA.

may miss important parts of the CNV, as segmentation may not cover the whole CNV volume, so data must be interpreted with care. Spaide et al.<sup>29</sup> focused, in a recent paper, on the importance of OCTA in understanding the vascular growth patterns and the changes induced by antiangiogenic treatments, observing signs of “abnormalization” of neovessels. This is a rather interesting concept, contradicting various theories of vascular normalization in eyes receiving intravitreal antiangiogenic injections. Moreover, Kuehlewein et al.<sup>18</sup> investigated the OCTA features of type 1 CNV and they described a neovascular complex, consisting of a feeder vessel

(Fig. 2A) and large branching vessels, which is resistant to anti-VEGF therapy. There are many ways type 1 CNV have been described in recent literature on OCTA, either as a “pruned tree” defined as an irregular, filamentous flow inside the neovascular network or as a high flow lesion in which new vessels can be either branching in a centrifuge manner from a central feeder vessel (“medusa pattern”) or can branch in one side of the feeder vessel (“seafan pattern”). A dark halo sometimes surrounds the lesion in the choriocapillaris segmentation, which could correspond either to a hypoperfusion of choriocapillaris or a fibrotic tissue<sup>18,30-32</sup> (Fig. 1H). In

**TABLE.** Statistical Results for Different Readers and Size Comparison Between OCTA and ICGA

	OCTA		ICGA		P Value*	P Value†	P Value‡	P Value§
	“Select Area”	“Vessel Area”	Intermediate	Late				
#1	2.21 ± 2.15	1.17 ± 1.10	2.70 ± 2.43	3.04 ± 2.38	0.02	0.0003	0.0001	0.0001
#2	2.03 ± 1.92	1.11 ± 0.99	2.71 ± 2.45	2.92 ± 2.55	0.002	0.0005	0.0001	0.0001

OCTA (( Select area )): total area of user-defined region of interest (mm<sup>2</sup>); (( Vessel area )): total area of vessels with flow (mm<sup>2</sup>); #1: first reader; #2: second reader; ICGA: indocyanine green angiography; Intermediate: lesion size measured between 3’ and 5’ (mm<sup>2</sup>); Late: lesion size measured between 30’ and 35’ (mm<sup>2</sup>).

\* Comparison between “Select area” and “Intermediate ICGA” via Wilcoxon signed-rank test.

† Comparison between “Select area” and “Late ICGA” via Wilcoxon signed-rank test.

‡ Comparison between “Vessel area” and “Intermediate ICGA” via Wilcoxon signed-rank test.

§ Comparison between “Vessel area” and “Late ICGA” via Wilcoxon signed-rank test.

our study, we analyzed the OCTA features of type 1 CNV in both treated and treatment-naïve patients, focusing on the lesion's neovascular size, as measured on ICGA and OCTA. In order to compare the entire neovascular complex in two different kinds of imaging, we measured the lesion area in the intermediate and late frames of ICGA and the flow area and vessel area in the choriocapillaris segmentation of OCTA. We also performed an image overlay. Only the images with a perfect overlap were analyzed. The statistical analysis revealed that for treated and treatment-naïve patients the lesion size in OCTA is significantly smaller than the lesion size measured in both intermediate and late frames of ICGA.

It is notable that the mean lesion size measured on intermediate phase of ICGA was significantly lower than the lesion size measured on late phase of ICGA. Despite the principle of ICGA, this finding raises the question of a possible leakage of the dye on late phase of ICG and then raises the question of the reliability of ICGA for quantitative evaluation of the neovascular membrane.

On the other hand, OCTA revealed a size of the neovascular membrane smaller than both intermediate and late phase of ICG. We can hypothesize either that OCTA underestimate the lesion size, or ICG overestimated the real size of the CNV. We support the hypothesis that OCTA could show the actual minimal surface of type 1 CNV, because a non-dye examination is not influenced by phenomenon of leakage. However, it is also possible that attenuation from the RPE generates a smaller lesion area on OCTA images.<sup>35</sup>

Our study has several limitations. On one hand, the retinal cube explored in OCTA covers limited areas of the fundus of 3 × 3 mm, which compelled us to analyze only small size type 1 CNV. On the other hand, all measurements were made with area-measuring software embedded on each instrument, in a real life clinical setting. All, in all, further improvements in the technique are needed, in order to overcome these limitations in the future.

In our study, we confirm the high reproducibility of the quantification of CNV on OCTA.<sup>34,35</sup> This supports the idea that OCTA could be considered for evaluation of the neovascular lesion area and the new vessels area and for evaluation of therapeutic responses.<sup>36,37</sup>

### Acknowledgments

Disclosure: **E. Costanzo**, None; **A. Miere**, None; **G. Querques**, Allergan, Inc. (C), Alimera Sciences, Inc. (C), Bayer Schering Pharma (C), Bausch & Lomb (C), Heidelberg (C), Novartis Pharmaceuticals Corporation (C); **V. Capuano**, None; **C. Jung**, None; **E.H. Souied**, Allergan, Inc. (C), Bayer Schering Pharma (C), Bausch & Lomb (C), Novartis Pharmaceuticals Corporation (C), Thea (C)

### References

- Bressler NM, Bressler SB, Fine SL. Age-related macular degeneration. *Surv Ophthalmol*. 1988;32:375-413.
- Gass JD, Norton EW, Justice J Jr. Serous detachment of the retinal pigment epithelium. *Trans Am Acad Ophthalmol Otolaryngol*. 1966;70:990-1015.
- Gass JD. Biomicroscopic and histopathologic considerations regarding the feasibility of surgical excision of subfoveal neovascular membranes. *Am J Ophthalmol*. 1994;118:285-298.
- Jung JJ, Chen CY, Mrejen S, et al. The incidence of neovascular subtypes in newly diagnosed neovascular age-related macular degeneration. *Am J Ophthalmol*. 2014;158:769-779.
- Sandhu SS, Talks SJ. Correlation of optical coherence tomography, with or without additional colour fundus

- photography, with stereo fundus fluorescein angiography in diagnosing choroidal neovascular membranes. *Br J Ophthalmol*. 2005;89:967-970.
- Pece A, Sannace C, Menchini U, et al. Fluorescein angiography and indocyanine green angiography for identifying occult choroidal neovascularization in age-related macular degeneration. *Eur J Ophthalmol*. 2005;15:759-763.
- Yannuzzi LA, Slakter JS, Sorenson JA, Guyer DR, Orlock DA. Digital indocyanine green videoangiography and choroidal neovascularization. *Retina*. 1992;12:191-223.
- Coscas F, Coscas G, Souied E, Tick S, Soubrane G. Optical coherence tomography identification of occult choroidal neovascularization in age-related macular degeneration. *Am J Ophthalmol*. 2007;144:592-599.
- Wilde C, Patel M, Lakshmanan A, Amankwah R, Dhar-Munshi S, Amoaku W; Medscape. The diagnostic accuracy of spectral-domain optical coherence tomography for neovascular age-related macular degeneration: a comparison with fundus fluorescein angiography. *Eye (Lond)*. 2015;29:602-609.
- Reichel E, Duker JS, Puliafito CA. Indocyanine green angiography and choroidal neovascularization obscured by hemorrhage. *Ophthalmology*. 1995;102:1871-1876.
- Guyer DR, Yannuzzi LA, Slakter JS, Sorenson JA, Hope-Ross M, Orlock DR. Digital indocyanine-green videoangiography of occult choroidal neovascularization. *Ophthalmology*. 1994;101:1727-1735.
- Yannuzzi LA. Indocyanine green angiography: a perspective on use in the clinical setting. *Am J Ophthalmol*. 2011;151:745-751.
- Guyer DR, Yannuzzi LA, Slakter JS, et al. Classification of choroidal neovascularization by digital indocyanine green videoangiography. *Ophthalmology*. 1996;103:2054-2060.
- Hee MR, Bauman CR, Puliafito CA, et al. Optical coherence tomography of age-related macular degeneration and choroidal neovascularization. *Ophthalmology*. 1996;103:1260-1270.
- Giani A, Luiselli C, Esmaili DD, et al. Spectral-domain optical coherence tomography as an indicator of fluorescein angiography leakage from choroidal neovascularization. *Invest Ophthalmol Vis Sci*. 2011;52:5579-5586.
- Jia Y, Bailey ST, Wilson DJ, et al. Quantitative optical coherence tomography angiography of choroidal neovascularization in age-related macular degeneration. *Ophthalmology*. 2014;121:1435-1444.
- Jia Y, Tan O, Tokayer J, et al. Split-spectrum amplitude-decorrelation angiography with optical coherence tomography. *Opt Express*. 2012;20:4710-4725.
- Kuehlewein L, Bansal M, Lenis TL, et al. Optical coherence tomography angiography of type 1 neovascularization in age-related macular degeneration. *Am J Ophthalmol*. 2015;160:739-748.
- Baker KJ. Binding of sulfobromophthalein (BSP) sodium and indocyanine green (ICG) by plasma alpha-1 lipoproteins. *Proc Soc Exp Biol Med*. 1966;122:957-963.
- Ryan SJ, Schachat AP, Wilkinson CP, Hinton DH, Sadda SR, Wiedemann P. Volume I. Retinal Imaging and Diagnostics; Basic Science and Translation to Therapy. *Retina*. 5th ed. 2013.
- Lim JI, Flower RW. Indocyanine green angiography. *Int Ophthalmol Clin*. 1995;35:59-70.
- Coscas G, Coscas F, Zourdani A. Atlas of indocyanine green angiography, fluorescein angiography, ICG angiography and OCT correlations. Paris: Elsevier; 2005.
- Spaide RF, Fujimoto JG, Waheed NK. Image artifacts in optical coherence tomography angiography. *Retina*. 2015;35:2163-2180.
- Regillo CD, Benson WE, Maguire JI, et al. Indocyanine green angiography and occult choroidal neovascularization. *Ophthalmology*. 1994;101:280-288.

25. Rush RB, Rush SW, Aragon AV II, Ysasaga JE. Evaluation of choroidal neovascularization with indocyanine green angiography in neovascular age-related macular degeneration subjects undergoing intravitreal bevacizumab therapy. *Am J Ophthalmol*. 2014;158:337-344.
26. Querques G, Tran TH, Forte R, Querques L, Bandello F, Souied EH. Anatomic response of occult choroidal neovascularization to intravitreal ranibizumab: a study by indocyanine green angiography. *Graefes Arch Clin Exp Ophthalmol*. 2012;250:479-484.
27. Stanga PE, Lim JI, Hamilton P. Indocyanine green angiography in chorioretinal diseases: indications and interpretation. *Ophthalmology*. 2003;110:15-21.
28. Ho AC, Yannuzzi LA, Guyer DR, Slakter JS, Sorenson JA, Orlock DA. Intraretinal leakage of indocyanine green dye. *Ophthalmology*. 1994;101:534-541.
29. Spaide RF. Optical coherence tomography angiography signs of vascular abnormalization with antiangiogenic therapy for choroidal neovascularization. *Am J Ophthalmol*. 2015;160:6-16.
30. Moulton E, Choi W, Waheed NK, et al. Ultrahigh-speed swept-source OCT angiography in exudative AMD. *Ophthalmic Surg Lasers Imaging Retina*. 2014;45:496-505.
31. Miere A, Semoun O, Cohen SY, et al. Optical coherence tomography angiography features of subretinal fibrosis in age-related macular degeneration. *Retina*. 2015;35:2275-2284.
32. Teussink MM, Breukink MB, van Grinsven MJ, et al. Angiography compared to fluorescein and indocyanine green angiography in chronic central serous chorioretinopathy. *Invest Ophthalmol Vis Sci*. 2015;56:5229-5237.
33. Novais EA, Adhi M, Moulton EM, et al. Choroidal neovascularization analyzed on ultrahigh-speed swept-source optical coherence tomography angiography compared to spectral-domain optical coherence tomography angiography. *Am J Ophthalmol*. 2016;164:80-88.
34. Bonini Filho MA, de Carlo TE, Ferrara D, et al. Association of choroidal neovascularization and central serous chorioretinopathy with optical coherence tomography angiography. *JAMA Ophthalmol*. 2015;133:899-906.
35. de Carlo TE, Bonini Filho MA, Chin AT, et al. Spectral-domain optical coherence tomography angiography of choroidal neovascularization. *Ophthalmology*. 2015;122:1228-1238.
36. Ferrara D, Waheed NK, Duker JS. Investigating the choriocapillaris and choroidal vasculature with new optical coherence tomography technologies. *Prog Retin Eye Res*. 2015;52:130-155.
37. Lumbroso B, Rispoli M, Savastano MC. Longitudinal optical coherence tomography-angiography study of type 2 naive choroidal neovascularization early response after treatment. *Retina*. 2015;35:2242-2251.